Structural Modification Changes the DNA Binding Mode of Cation-Substituted Anthraquinone Photonucleases: Association by Intercalation or Minor Groove Binding Determines the DNA Cleavage Efficiency†

David T. Breslin, Changjun Yu, Danith Ly, and Gary B. Schuster*

School of Chemistry and Biochemistry, Georgia Institute of Technology, Atlanta, Georgia 30332-0400

Received February 5, 1997; Revised Manuscript Received April 9, 1997⊗

ABSTRACT: The mode of binding anthraquinone derivatives, bearing positively charged ammonium side chains, to duplex DNA was investigated by optical and NMR spectroscopy. Absorption, circular dichroism, emission, and one- and two-dimensional homonuclear NMR spectroscopy show that mono- and dication-substituted quinones, AQS and 27AQS, bind primarily by intercalation. In contrast, these experiments indicate that the tetracationic anthraquinone 27AQS2 is bound nonintercalatively to duplex DNA. In particular, analysis of the NMR spectrum of 27AQS2 bound to a specially designed synthetic self-complementary dodecanucleotide (5′-CGCGAATTCGCG-3′) shows it to be associated primarily with the minor groove of the central AATT sequence. The change in the DNA binding mode greatly affects the photophysical and photochemical properties of these photonucleases with DNA.

Numerous compounds, of varying size, and from structurally diverse groups, bind to duplex DNA and cause physical or chemical modification of the structure of the polymer. Often, these chemical modifications result in strand cleavage and fragmentation of the DNA into shorter segments. This process is a valuable tool for biochemical manipulation if the site of cleavage depends on the base sequence. Selective targeting of specific sequences or structural motifs for cleavage permits development of useful artificial nucleases (Pratviel et al., 1995; Sigman et al., 1993) or therapeutic agents. Alternatively, inducible, completely random cleavage of DNA provides a means of identifying binding sites for small ligands through footprinting experiments (Breiner et al., 1995; Jeppesen & Nielsen, 1988; Uchida et al., 1989).

Recently, there has been increased interest in the discovery and investigation of compounds that cleave DNA when irradiated with visible or UV light (Sitlani et al., 1992; Nielsen et al., 1992; Hertzberg & Dervan, 1984; Liang et al., 1994; Ranganathan et al., 1994; Riordan & Wei, 1994; Takasaki & Chin, 1994; Schnaith et al., 1994; Nagai et al., 1991; Nicolau et al., 1990; Neyhart et al., 1993). Photonucleases are especially convenient because they are inert until activated by light. Since light is applied externally to the reaction "vessel", it can readily be controlled spatially and temporally. The photonucleases discovered so far operate by several distinct mechanisms. In one class, excitation of a photosensitizer generates a freely diffusing intermediate species, such as singlet oxygen (Cadet et al., 1986; Floyd et al., 1989), or hydroxyl radical (Tullius et al., 1987; Hertzberg & Dervan, 1982; Saito et al., 1990), that reacts with DNA when it encounters a suitable functional group. In a second class, the photonuclease is bound before its activation, there is no diffusible species, and damage is localized at or near the binding site (Nielsen, 1991; Cheng et al., 1995; Sigman, 1986; Barton, 1986; Stubbe & Kozarich, 1987; Hertzberg & Dervan, 1982). Photonucleases, like any other small DNA ligand, can associate by intercalation or by fitting into one of the grooves. Importantly, the type and efficiency of the light-initiated cleavage reaction will depend on the binding site that the photonuclease occupies.

Photosensitized chemical modification of DNA eventually leading to strand cleavage can be initiated, in principle, by hydrolysis of a sugar−phosphate bond (Takasaki & Chin, 1994; Siebenlist et al., 1980), hydrogen atom abstraction from a sugar or nucleotide base (Pratviel et al., 1995; Stubbe & Kozarich, 1987; Papavassiliou, 1995), cycloaddition of singlet oxygen to a nucleotide base (Sheu & Foote, 1995; Raoul & Cadet, 1996), or one-electron oxidation of a nucleotide base (Cullis et al., 1996; Jovanovic & Simic, 1986). For example, singlet oxygen reacts preferentially with the guanine bases, leading to their degradation and subsequent selective cleavage at G-containing sequences after alkali treatment (Cadet, 1986; Floyd, 1989). In striking contrast, hydroxyl radical will abstract a hydrogen atom from a deoxyribose unit, giving spontaneous (no alkali treatment required) cleavage that is independent of the base identity (Tullius et al., 1987; Hertzberg & Dervan, 1982; Saito et al., 1990). Hydroxyl radical also will abstract a hydrogen atom from the methyl group of thymine, yielding additional alkali-requiring cleavage at T-containing sequences (Dizdaroglu, 1984). Irradiation of a compound that is intercalated in DNA often results in single-electron oxidation of an adjacent base and alkali-requiring cleavage whose efficiency is strongly dependent on the base sequence (Saito et al., 1995; Ito et al., 1993; Hall et al., 1996; Brun & Harriman, 1992).

We have been exploring the ability of a series of water soluble anthraquinone derivatives to function as photonucleases (Koch et al., 1993; Armitage et al., 1994; Breslin & Schuster, 1996; Ly et al., 1996). Three general classes of DNA scission that depend on the specific structure of the quinone have been observed. The first class is exemplified

† This work was supported by grants from the National Institutes of Health (RO1 GM28190 and PHS NRSA GM16498) and the National Science Foundation (CHE-9596166).

⊗ Abstract published in *Advance ACS Abstracts,* June 15, 1997.

S0006-2960(97)00275-4 CCC: $14.00

Chart 1

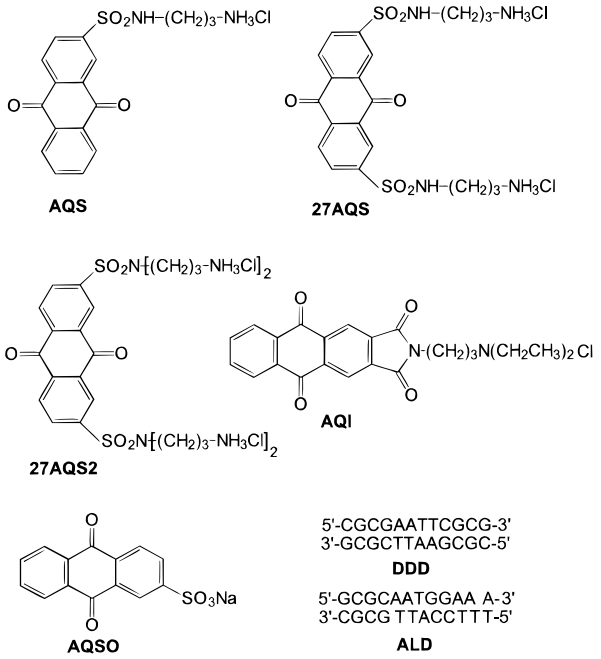

by AQS[1] (see Chart 1), which intercalates in DNA. Irradiation of the intercalated quinone initiates rapid electron transfer for formation of a base radical cation (hole) and the quinone radical anion. The hole is trapped by reaction with water or O_2 at a GG step, yielding alkali-requiring DNA cleavage predominantly at the 5′-G of this sequence. A second category of quinone reactivity is typified by AQI, which binds to the minor groove of DNA (Breslin et al., 1997). Irradiation of the AQI yields totally nonspecific spontaneous cleavage at every base presumably by hydrogen atom abstraction from a deoxyribose unit. A third category of quinone reactivity is displayed by AQSO (Armitage & Schuster, 1997), which, because of its negative charge, does not associate with DNA. Irradiation of AQSO in buffer solutions containing chloride ion generates a freely diffusible species which abstracts a hydrogen atom from the sugar backbone and causes spontaneous, nonselective cleavage of the DNA.

In this paper, we describe 27AQS2, a water soluble polyammonium-substituted anthraquinone derivative. Analysis of the association of 27AQS2 with DNA, particularly by NMR spectroscopy, shows that it binds in the minor groove of DNA at regions rich in A and T. Irradiation of 27AQS2 bound to DNA causes less efficient cleavage at GG steps than does irradiation of intercalated AQS.

RESULTS

(1) DNA Binding Constants of the Quinone Derivatives. All of the cation-substituted quinones examined bind to DNA with affinities that depend on the structure of the quinone and the sequence of the double-stranded DNA. The association constants of the quinones in PBS buffer with three different synthetic DNAs were measured by competitive titrations with fluorescent probes. Scatchard analysis of the data gives binding isotherms that were fit to the McGhee−VonHippel model (Armitage et al., 1994). Ethidium bromide was used to measure the association constants of the quinones with poly(dAdT)$_2$ and poly(dGdC)$_2$, while propidium bromide was used for poly(dA)·poly(dT) because of its higher binding constant. The results of this competitive binding study are compiled in Table 1.

Table 1: Association Constants of the Anthraquinone Photonucleases with Various DNA Polymers in PBS Solution

	K_a (M^{-1}) × 10^4 [a]		
anthraquinone	poly(dAdT)$_2$	poly(dGdC)$_2$	poly(dA)·poly(dT)
AQS	23	4.8	0.35
27AQS	77	39	1.7
27AQS2	107	50	23

[a] The estimated error in the association constants is ±10%.

Table 2: Hypochromicity of Anthraquinone Photonucleases Induced by Various DNA Polymers

	% hypochromicity (% bound)[a]		
anthraquinone	poly(dAdT)$_2$	poly(dGdC)$_2$	poly(dA)·poly(dT)
AQS	27 (95)	23 (80)	7 (25)
27AQS	21 (98)	20 (97)	16 (62)
27AQS2	11 (99)	15 (98)	0 (95)

[a] The estimate of % bound is calculated from the binding constants listed in Table 1.

As expected, the association constants of the quinones increase considerably with the number of positive charges the structure bears. This effect is seen most dramatically for binding to poly(dA)·poly(dT), where the monocationic quinone, AQS, has an association constant that is ca. 65 times less than that of the tetracationic quinone 27AQS2. In contrast, the association constant change for the same two quinones is only a factor of ca. 5 for binding to poly(dAdT)$_2$.

The differential response of AQS and 27AQS2 to the variation in DNA structure suggests a different binding mode for these two quinones. Intercalation is more difficult in poly(dA)·poly(dT) than it is in poly(dAdT)$_2$ because of the bifurcated hydrogen bonds present in the former (Nelson et al., 1987). Consequently, the association constant for AQS, which binds by intercalation, is reduced considerably in poly(dA)·poly(dT). The much smaller change in the association constant for 27AQS2 with these two AT rich DNA polymers suggests that its binding does not disrupt the π stacking of the bases, as is required if intercalation is the primary binding mode. This observation is supported by other spectroscopic analyses of the binding of 27AQS2 to DNA.

(2) UV Spectra of Quinones Free and Bound to DNA. The binding of a molecule having a perturbable π-electron system to DNA typically results in a hypochromic and bathochromic shift in its absorption spectrum. This effect is usually more pronounced for compounds that bind by intercalation than for those that are associated with a groove (Wilson et al., 1989a,b, 1990). We measured the absorption spectra of the mono-, di-, and tetracationic quinones in PBS buffer containing the three different synthetic DNA polymers. Their absorption spectra were compared with those of the free quinones under identical conditions but in the absence of DNA at 327 nm where their extinction coefficients are similar. The UV spectral differences of the DNA−quinone complexes are compiled in Table 2.

[1] Abbreviations: 27AQS2, *N*,*N*,*N*,*N*′-tetrakis(3-aminopropyl)-2,7-anthraquinonedisulfonamide tetrahydrochloride; 27AQS, *N*,*N*′-bis(3-aminopropyl)-2,7-anthraquinonedisulfonamide dihydrochloride; AQS, *N*-(3-aminopropyl)-2-anthraquinonesulfonamide hydrochloride.

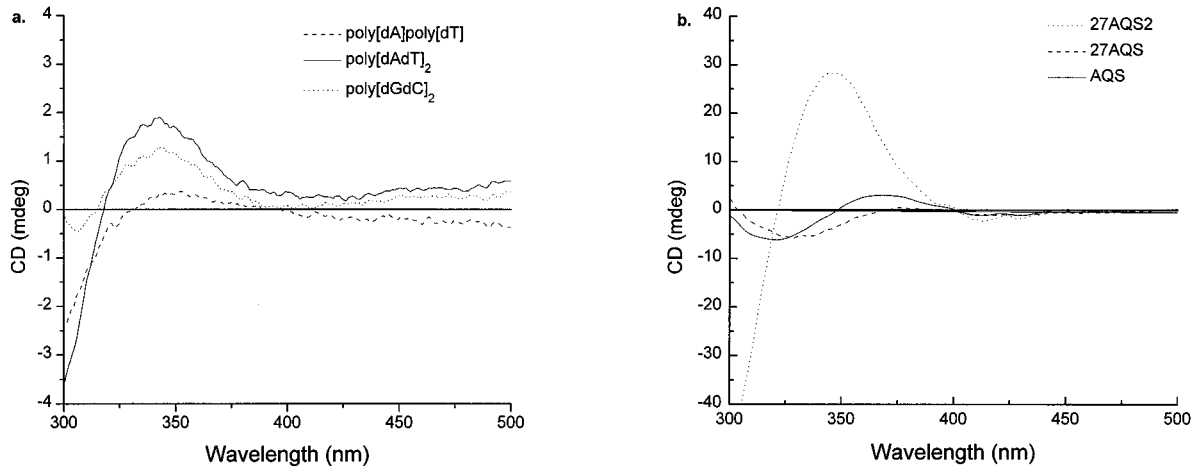

FIGURE 1: CD spectra of 27AQS2 induced by various DNA polymers. These spectra were recorded in PBS solutions containing 100 μM DNA (base pairs) with 20 μM anthraquinone in a 1 cm path length cell.

The DNA-induced hypochromicities of the monocationic intercalator, AQS, with poly(dAdT)$_2$ and poly(dGdC)$_2$ are roughly comparable. However, the hypochromicity of the tetracationic 27AQS2 is considerably reduced in both of these synthetic polymers. This finding suggests that the tetracationic quinone does not bind to DNA predominantly by intercalation. The changes in absorption spectra of the free and DNA-bound quinones are too weak to permit accurate determination of binding constants by UV spectroscopy.

(3) Induced CD Spectra of the DNA−Quinone Complexes. Achiral molecules bound to DNA often show induced circular dichroism spectra that reveal structural information about the complex. The shape and intensity of an induced CD spectrum is sensitive to the relative orientation of the bound molecule with respect to the DNA helix. In particular, groove-bound molecules generally exhibit a much greater induced CD signal intensity than do similar compounds when they are intercalated (Lyng et al., 1991a,b). The induced CD spectrum of tetracationic 27AQS2 with poly(dAdT)$_2$ is shown in Figure 1a. Significantly, the signal for monocationic AQS, which intercalates in poly(dAdT)$_2$, is so weak that it is not measurable at these concentrations.

The induced CD spectra of AQS, 27AQS, and 27AQS2 are measurable, at higher concentrations, when associated with a dodecanucleotide (DDD, see Chart 1) specially prepared for NMR analysis of DNA binding by these quinones (see below). These induced CD spectra, shown in Figure 1b, were recorded under conditions where each of the quinones is essentially completely bound (>90%) to the dodecamer. Significantly, intercalated AQS and 27AQS both exhibit nearly identically shaped, weak CD spectra. In contrast, the CD spectrum for the tetracation 27AQS2 is biphasic and ca. 10 times stronger than that for the mono- and dicationic quinones. These findings again indicate that 27AQS2 binds differently to DNA than does AQS or 27AQS.

(4) Phosphorescence of Anthraquinones Complexed with DNA. Many anthraquinone derivatives, particularly those having lowest-energy $n\pi^*$ triplet states, phosphoresce in frozen solution. Since diffusion does not occur under these conditions, quenching indicates preassociation of the quinone and its quencher. We observed that DNA effectively quenches the phosphorescence of the anthraquinone derivatives when they are intercalated (Koch et al., 1993; Armitage et al., 1994; Breslin & Schuster, 1996; Ly et al., 1996). Thus, the emissive behavior of the quinone−DNA complexes provides a convenient means of assessing the primary mode of association.

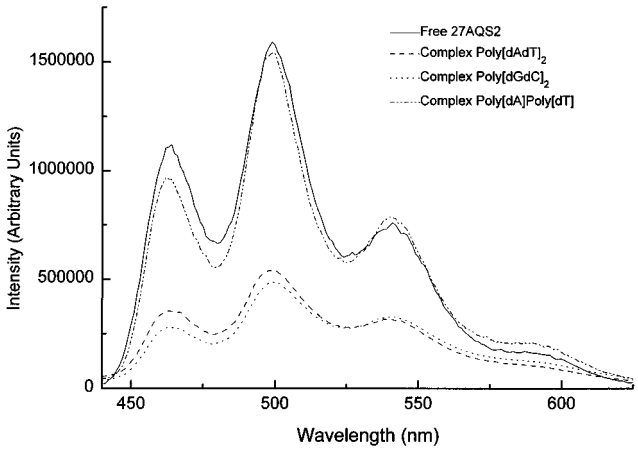

FIGURE 2: Phosphorescence spectra of free and DNA-bound 27AQS2. These spectra were recorded at 77 K in solutions of 50% PBS/50% glycol containing 100 μM DNA (base pairs) and 20 μM anthraquinone in a 1 cm path length cell.

The phosphorescence emissions of AQS, 27AQS, and 27AQS2 were measured at 77 K in a frozen solution of 50% ethylene glycol and 50% PBS. These emissions are strong; the spectra are typical of anthraquinones, and they are virtually identical to each other. The phosphorescence of these quinones responds differently to inclusion of DNA in the frozen solution. The quenching results are summarized in Table 5, and typical spectra are shown in Figure 2. Comparing the results from monocationic AQS−DNA complexes with those from the tetracationic 27AQS2−DNA complexes is especially revealing. Under the conditions of these experiments, the phosphorescence from AQS or 27AQS that is bound to poly(dAdT)$_2$, poly(dGdC)$_2$, or poly(dA)·poly(dT) is completely quenched. The small fraction of the emission that remains corresponds roughly to the amount of unbound quinone. This behavior is expected from an intercalation complex where electron transfer from a base to the excited state of the quinone will be rapid compared with the phosphorescence emission. In contrast, the phosphorescence of 27AQS2 bound to poly(dAdT)$_2$ or poly(dGdC)$_2$ is only partially quenched, and its emission is essentially unaffected by binding to poly(dA)·poly(dT). The absence of excited state quenching clearly demonstrates that 27AQS2 does not bind to poly(dA)·poly(dT) by intercalation.

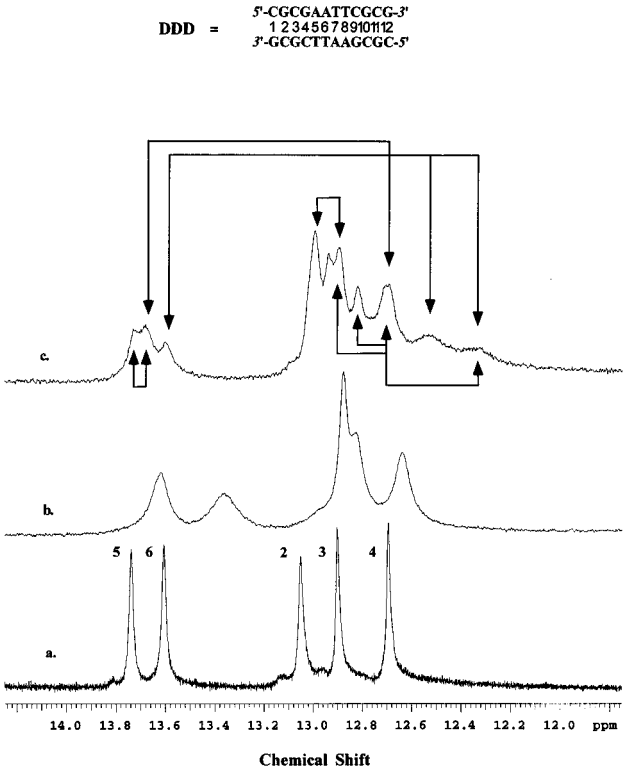

FIGURE 3: Imino proton region of DDD complexed with AQS and 27AQS2. The PBS solutions were prepared to contain the anthraquinone and duplex dodecamer in a 1:1 ratio: (a) free dodecamer, (b) AQS complex, and (c) 27AQS2 complex.

(5) NMR Studies of the Complexes of AQS and 27AQS2 with Duplex DDD. The duplex dodecamer DDD is often used for analysis of the binding of small molecules to DNA. The sequence is long enough to have more than one turn of the helix and sufficient to bind more than one ligand (Patel et al., 1981). The alternating GC sequence provides sites for intercalation, while the interior AATT sequence is adequate for groove binders.

Analysis of ligand binding by NMR spectroscopy requires the assignment of individual resonances of the native duplex structure and correlating those assignments to that of the shifted resonances when a ligand is bound. Fortunately, the proton resonances for native DDD have been previously assigned (Hare et al., 1983), and the shifts caused by ligands that bind to a groove or intercalate in this structure have been thoroughly characterized. We recorded the ^{1}H NMR spectra of the imino protons (exchangeable) and the nonexchangeable protons of DDD with bound AQS or 27AQS2. As is often the unfortunate case (Eriksson et al., 1994), an intermediate rate of exchange does not permit the acquisition of high-resolution NMR spectra for these quinones bound to DDD. Nevertheless, these spectra are adequate to show that AQS intercalates and that 27AQS2 binds to DDD in the minor groove, probably, at the central AATT sequence.

(a) Exchangeable (Imino) Protons. The NMR spectra of the imino protons of the dodecamer DDD and its complexes with AQS and 27AQS2 were recorded in an 85% H_2O/15% D_2O buffer solution. These protons of the uncomplexed oligonucleotide give signals in the region from 11 to 14 ppm (Figure 3a). Due to the symmetry of the uncomplexed dodecamer, there are only six unique imino proton resonances. Of these, five are sharp singlets and one, the terminal GC, is broadened presumably as a consequence of fraying at the ends. The five sharp resonances of the imino protons have been assigned as is indicated in Figure 3a (Gräslund et al., 1992). The furthest downfield signals are attributed to the imino protons of the central TTAA sequence, and the three upfield resonances are assigned to the flanking CGC sequences. The terminal GC base pair appears to be a broad signal centered at ca. 13.08 ppm.

The effects of association of AQS with DDD are readily apparent in the NMR spectra of the imino protons, and they are relatively simple to interpret. The spectrum recorded at a 1:1 ratio of quinone to dodecamer is shown in Figure 3b. The most significant changes to the spectrum caused by binding of AQS are line broadening and a slight upfield shift of each resonance. The observable imino protons of the complex with AQS were assigned by determining the adjacencies from nuclear Overhauser effects (NOE). These assignments and the chemical shifts of the imino protons of the complex are reported in Table 3.

Significantly, since the spectral complexity of the imino protons for the free dodecanucleotide does not increase, the symmetry of DDD must be maintained when AQS is intercalated. This is a consequence of signal averaging by exchange of bound and free AQS on the NMR time scale. We have shown previously by stopped-flow measurements that AQS dissociates from DNA in less than 1 ms (Armitage et al., 1994). Furthermore, since each of the observable imino protons is shifted upfield, intercalation of AQS in every possible site must occur. This is consistent with our previous finding that the association constants of monocation-substituted anthraquinones are independent of whether a sequence contains a GG step.

The complexity of the imino proton spectra of DDD increases markedly, and the quality of the spectra that can be obtained declines further when 27AQS2 is bound to the oligonucleotide. The spectrum recorded at a 1:1 ratio of 27AQS2 to DDD is shown in Figure 3c. An unambiguous spectral change is the fact that the symmetry of the free oligonucleotide has been lost. Many of the observable imino proton signals are doubled, and there are 10 resolvable resonances in this region when 27AQS2 is bound to the oligonucleotide. This reduced signal averaging is consistent with our previous finding from stopped-flow measurements that the dissociation of the tetracation-substituted quinones from DNA has a half-life of approximately 180 ms.

Analysis of the gross structure of 27AQS2 bound to DDD is facilitated by identification of neighboring imino protons from analysis of the NOE in 15% D_2O at 30 °C. The identified adjacencies are indicated by arrows linking the appropriate resonances on Figure 3c. Closer inspection of Figure 3c reveals that the intensities of the AT imino protons are diminished relative to the signals for the GC imino protons. And, most significantly, two new temperature-sensitive signals appear upfield of the signals in the uncomplexed dodecanucleotide. These resonances are broad at 30 °C, but they sharpen somewhat when the complex is cooled to 10 °C (data not shown). Inspection of Figure 3c indicates beyond question that 27AQS2 is bound to DDD differently than AQS. In particular, the tetracation-substituted quinone appears to bind preferentially in the AT region. Additional analysis of this spectrum and the structure of the bound complex is presented in the Discussion.

(c) Sugar and Nonexchangeable Base Protons. The ^{1}H NMR spectrum of DDD recorded in 100% D_2O PBS buffer

Table 3: Assignment of NMR Resonances for DDD with AQS Bound

	chemical shift (δ) and $\Delta\delta$ in parentheses					
base	H8	H6	H5	CH3	C1′H	imino
C_1		7.52 (−0.07)	5.74 (−0.10)		5.65 (−0.06)	broad
G_2	7.84 (−0.08)				5.53 (−0.31)	12.87 (−0.18)
C_3		7.14 (−0.10)	5.29 (−0.06)		5.47 (−0.08)	12.78 (−0.11)
G_4	7.71 (−0.12)				5.28 (−0.14)	12.63 (−0.06)
A_5	8.03 (−0.06)				5.82 (−0.14)	13.59 (−0.14)
A_6	8.03 (−0.06)				6.01 (−0.13)	13.35 (−0.23)
T_7		7.09 (−0.02)		1.23 (−0.01)	5.84 (−0.05)	
T_8		7.20 (−0.07)		1.44 (−0.07)	5.96 (−0.12)	
C_9		7.35 (−0.09)	5.58 (−0.03)		5.63 (−0.04)	
G_{10}	7.79 (−0.10)				5.51 (−0.32)	
C_{11}		7.22 (−0.08)	5.32 (−0.09)		5.63 (−0.10)	
G_{12}	7.82 (−0.08)				6.01 (−0.09)	

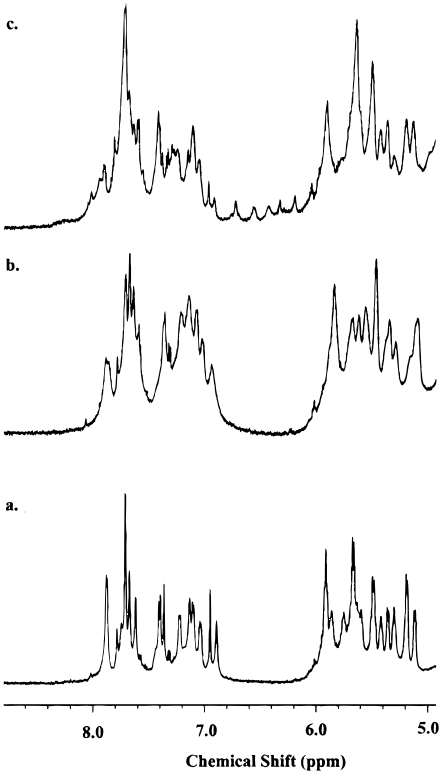

FIGURE 4: Regions of the one-dimensional spectra for the nonexchangeable protons of DDD complexed with AQS and 27AQS2. The PBS solutions were prepared to contain the anthraquinone and duplex dodecamer in a 1:1 ratio: (a) free dodecamer, (b) AQS complex, and (c) 27AQS2 complex.

gives resonances that are relatively sharp. The portion of this spectrum from 5.0 to 8.5 ppm is shown in Figure 4a. A homonuclear two-dimensional NOESY experiment confirms previous assignments (Hare et al., 1983).

The NMR absorptions of the sugar and nonexchangeable base protons of DDD are broadened and shifted when AQS is introduced into the dodecamer, but the number of observable NMR signals remains unchanged. This is consistent with the equilibrium binding results, described above, that indicate rapid exchange of the anthraquinone ligand between different binding sites that is faster than the NMR time scale. The spectrum of DDD with AQS bound is shown in Figure 4b. Each of the resonances is readily assigned by following connectivities obtained from a homonuclear ^{1}H NOESY experiment using the standard protocol. Each of the aromatic protons (H8 on A and G, H5 and H6 on C, and H6 on T) and every C1′ proton of the deoxyribose groups are shifted upfield between 0.1 and 0.2 ppm. The assigned chemical shift data for the AQS association complex are summarized in Table 3.

We are unable to assign specific signals to the aromatic resonances of the AQS skeleton. These signals evidently overlap the spectral region covered by the aromatic protons of the oligomer. No cross-peaks between the quinone and dodecamer are detectable in the two-dimensional spectra that indicate points of close contact.

The ^{1}H NMR spectrum of the tetracationic 27AQS2 complexed with DDD recorded at 10 °C and a 1:1 ratio of quinone to dodecanucleotide is shown in Figure 4c. Despite the low quality of the obtainable spectra, examination of them reveals a significant difference with respect to that of AQS bound to the dodecanucleotide. First, a new set of signals appears between δ 6.25 and 6.85 ppm where there are no absorptions of free DDD or when it is complexed with AQS. These signals broaden, and they lose their intensity when the sample is warmed. In addition, a very broad, low-intensity signal can be seen in this spectrum in the region from δ 8.4 to 8.1 ppm.

A NOESY experiment was performed to assign the resonances of the DDD complex with 27AQS2. Comparisons of selected regions of these spectra with those of the corresponding AQS−DDD complex are shown in Figure 5. We find that the two-dimensional spectra of the 27AQS2−DDD complex in the region of the AT base pairs are changed the most.

The portions of the NOESY spectra showing the cross-peaks of the T-methyl, C2′, and C2″ sugar protons with the nucleotide aromatic protons of the DDD complexes with AQS and with 27AQS2 are shown in panels a and b of Figure 5, respectively. The cross-peaks from the GC and AT base pairs of the AQS complex are relatively strong, and there is complete correspondence between these signals and those from uncomplexed DDD. In contrast, with 27AQS2, the signals arising from the AT base pairs are significantly perturbed compared to those of free DDD or when it is complexed with AQS. There are four clearly resolved signals that appear in the T-methyl region. The furthest upfield signal at 1.23 ppm corresponds to an unperturbed resonance from the T_7 methyl. The signals at 1.50 ppm are cross-peaks of an unaffected T_8 methyl group with the C6 of T_8 (7.32 ppm) and T_7 (7.08 ppm). The final two methyl signals are unique to this complex, and they are found slightly downfield from the unperturbed T_8 methyl. Both of the new methyl resonances have NOE interactions with two different base protons. Finally, a new cross-peak is observed at 3.26 ppm on the sugar proton axis and 7.82 ppm on the aromatic

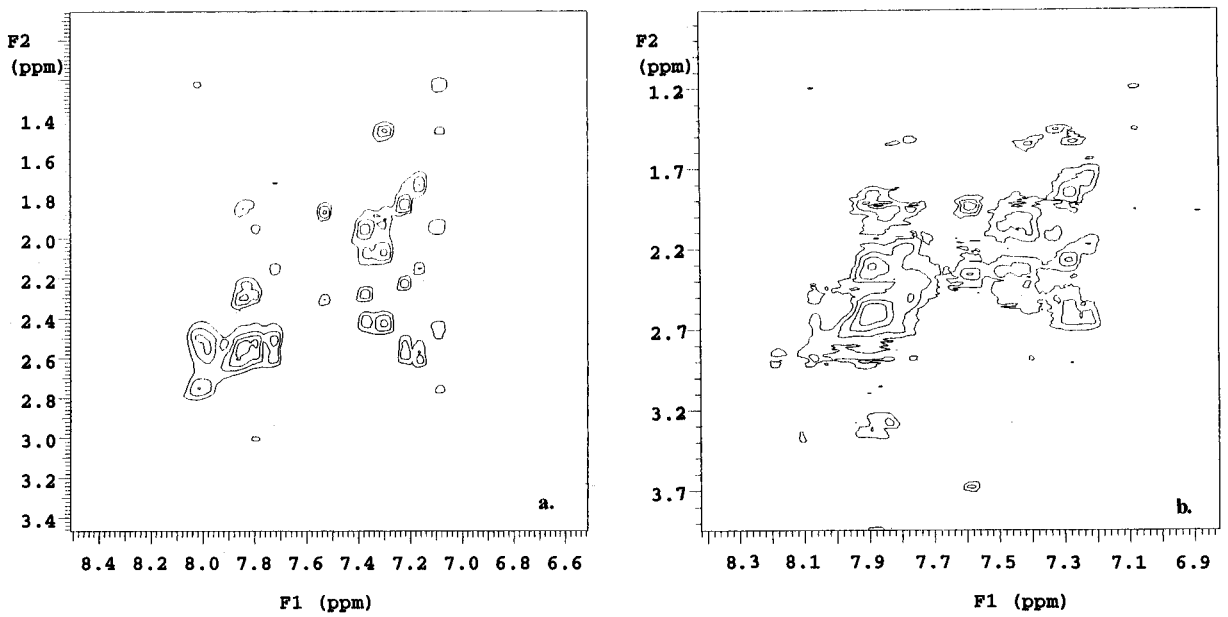

FIGURE 5: NOESY proton spectra, T-methyl, C2′, and C2″ with the nucleotide aromatic protons region, of DDD complexed with (a) AQS and (b) 27AQS2.

axis. The complexity observed in the NOESY spectrum of complexed 27AQS2 is probably due to slow exchange kinetics or the formation of two or more distinct complexes. These data indicate that 27AQS2 interacts most strongly at the central AATT stretch, since this is the area of greatest change of the NMR signals.

(6) Photocleavage of DNA by AQS and 27AQS2. Irradiation of intercalated anthraquinone derivatives typically leads to cleavage of DNA selectively at the 5′-G of GG steps. The efficiency of cleavage at a GG step is controlled, in part, by the base sequence surrounding it. We probed the ability of AQS and 27AQS2 to cleave an identical segment of DNA by irradiating their complexes with the dodecamer ALD (see Chart 1). This oligonucleotide contains one of the sequences we have found to be cleaved most efficiently (Ly et al., 1996).

Irradiated samples of ALD complexed with AQS or 27AQS2 were treated with piperidine and then 5′-dephosphorylated with bacterial alkaline phosphatase. The oligonucleotide products were separated by HPLC, and 5′-GCGCAAT-3′, from 5′-G cleavage, and 5′-GCGCAATG-3′, from 3′-G cleavage, were identified by comparison with authentic samples. The quantum yields for DNA cleavage were determined using an anthraquinone-2,6-disulfonate actinometer (Ly et al., 1996). The results are summarized in Table 6. Significantly, cleavage by 27AQS2 is only ca. 15% as efficient as cleavage by AQS. Since the properties of the excited states of these quinones are essentially identical, this change in efficiency must be caused by differences in their binding modes.

Table 4: Assignment of NMR Resonances for DDD with 27AQS2 Bound

	chemical shift (δ) and $\Delta\delta$ in parentheses				
base	H8	H6	H5	CH3	C1′H
C_1		7.60 (0.01)	5.83 (−0.01)		5.69 (−0.02)
G_2	7.91 (0.01)				5.84 (0.0)
C_3		7.23 (−0.01)	5.33 (−0.02)		5.57 (0.02)
G_4	7.94 (0.11)				5.32 (−0.10)
A_5	na[a]				na
A_6	na				na
T_7		na		na	na
T_8		na		na	na
C_9		7.62 (0.18)	5.62 (0.01)		5.40 (−0.27)
G_{10}	7.88 (−0.01)				5.82 (0.0)
C_{11}		7.30 (0.0)	5.37 (−0.03)		5.72 (−0.01)
G_{12}	7.89 (−0.01)				6.11 (0.01)

[a] na = not assigned.

Table 5: Phosphorescence Quenching of Anthraquinone Photonucleases by Various DNA Polymers at 77 K[a]

	% phosphorescence quenching (% bound)[a]		
anthraquinone	poly(dAdT)$_2$	poly(dGdC)$_2$	poly(dA)·poly(dT)
AQS	85 (90)	60 (68)	10 (15)
27AQS	95 (97)	92 (94)	37 (44)
27AQS2	67 (98)	67 (95)	0 (90)

[a] The measurements were done in 50% aqueous PBS/50% ethylene glycol. Samples were excited at 327 nm. The parenthetical values indicate the % of the quinone bound to DNA assuming that the presence of ethylene glycol does not effect the association constant listed in Table 1.

DISCUSSION

The considerable interest in the interactions of anthraquinone derivatives with DNA is spurred, in part, by drugs and potential drug candidates that have anthraquinone units as part of their structure. Our investigation of this class has identified a series of compounds that bind to DNA and cause oxidative damage that leads to cleavage when irradiated with UV light. In particular, AQS and other monocationic derivatives bind to DNA by intercalation and give the relatively efficient 5′-G selective cleavage described above. It appears that the dication-substituted anthraquinone derivative, 27AQS, also intercalates in DNA and similarly gives 5′-G selective cleavage when irradiated. We were surprised to discover that the tetracation-substituted derivative, 27AQS2, behaves differently. The experiments reported above indicate that this structural change causes a switch in the association mode for 27AQS2 which affects its photochemical reactions with DNA.

Table 6: Efficiency for GG Selective Cleavage of ALD with Various Quinones

anthraquinone	product yields (μM) 3-mer	4-mer	cleavage selectivity[a] (5′ cleavage:3′ cleavage)	$\Phi_{GG} \times 10^{-4}$
AQS	2.0 ± 0.1	19.6 ± 3.9	90:10	54
27AQS2	1.3 ± 0.6	5.2 ± 1.7	75:25	8.0

[a] The error for cleavage selectivity by AQS is ±8 and by 27AQS2 is ±15.

(1) Spectral Evidence Showing That AQS and 27AQS Intercalate in DNA and 27AQS2 Does Not. 27AQS2 is more tightly bound to DNA than either AQS or 27AQS as shown by the competitive binding studies. This greater attraction is a consequence of the greater number of positive charges that the tetracation bears. Intercalative DNA binding for the monocationic AQS is supported by the optical and NMR spectroscopic data presented herein. Furthermore, recent aqueous solution viscometric measurements and atomic force microscopy experiments (Coury et al., 1997) show lengthening of the DNA by AQS as it is unwound by the intercalated quinone. Comparison of AQS and 27AQS2 by optical and NMR spectroscopy shows that the tetracation associates with DNA by a unique mode. This conclusion is supported by several sets of experiments outlined below.

(a) UV Spectroscopy. The hypochromic effect induced by the DNA on the spectrum of a bound ligand is one indicator of the binding mode. In general, intercalators have stronger hypochromicities than the corresponding groove binders. The data in Table 2 show that AQS and the dication 27AQS exhibit hypochromicities of ca. 25% when bound to poly(dAdT)$_2$ or to poly(dGdC)$_2$ but that the tetracationic 27AQS2 has a hypochromic effect of only ca. 10% when bound to these polymers. The same trend in hypochromicities is observed for this series of anthraquinones with poly(dA)·poly(dT). The much lower effect with this DNA polymer is due to the reduced binding affinities. After correction for the unbound fraction of quinone, AQS and 27AQS experience an approximately 25% decrease in absorbance when bound to poly(dA)·poly(dT), while 27AQS2 exhibits a negligible effect [hypochromicity is calculated by $H_{red} = H_{obs}$/(fraction bound), where H_{red} = reduced hypochromicity, H_{obs} = observed hypochromicity, and the fraction bound comes from Table 1]. Thus, the absorption spectra of the complexes agree with assignment of a groove binding mode for 27AQS2, and intercalation for AQS and 27AQS.

(b) CD Spectroscopy. The shape and intensity of an induced CD spectrum provide information on the orientation of a bound chromophore with respect to the DNA helix. In particular, the CD spectra for AQS and dicationic 27AQS when associated with DDD are of similar intensity and shape, but the spectrum of 27AQS2 is 1 order of magnitude stronger. Ligands associated in the DNA grooves are known to have CD signals approximately 10 times greater than those of similar intercalating chromophores (Lyng et al., 1991a,b).

The induced CD spectrum of 27AQS2 has a different shape than the mono- or dicationic quinones. The especially strong biphasic spectrum for 27AQS2 bound to poly(dA)·poly(dT) is nearly identical with its CD spectrum when bound to DDD. In contrast, the CD spectra of 27AQS2 bound to poly(dAdT)$_2$ and poly(dGdC)$_2$ show only one lobe. This finding suggests that the tetracation is bound to the central AT region of the dodecamer in a geometry resembling that found with the nonalternating DNA polymer.

(c) NMR Spectroscopy. The NMR spectra of AQS and 27AQS2 complexed with DDD are quite complex, compromised by an intermediate exchange rate, but provide sufficient additional information to assist in assignment of differential binding modes for AQS and 27AQS2. An analysis of the relatively simple imino proton region is informative since the effect of 27AQS2 binding on the NMR spectrum of the exchangeable imino protons can be used to construct several possible binding models using the known intercalator AQS for comparison. With this logic, we can eliminate intercalation as the primary association mode for 27AQS2.

Binding of AQS causes upfield shifts for all of the nucleotide base, C1′ sugar, and imino proton resonances of the dodecanucleotide. These shifts are a consequence of intercalative binding. Several intercalators such as daunomycin, an anthraquinone-based antibiotic (Phillips & Roberts, 1980), actinomycin (Patel et al., 1981), and DAPI (Wilson et al., 1989a,b) have been studied by NMR techniques. In all of these instances, even with unfused aromatic intercalators (Wilson et al., 1989a,b), binding causes the imino protons to shift upfield. The magnitude of the shift depends primarily on the strength of the ring current associated with the intercalator. Acridines possess large magnetic anisotropies and cause large shifts in DNA signals. Anthraquinones typically produce much smaller perturbations on the DNA resonances because the π-electron system is less polarizable. The similar magnitude of the upfield shift for each base pair of the dodecamer indicates that association of AQS occurs at many or all of the possible intercalation sites. The absence of signal doubling due to a loss of symmetry shows that AQS is in fast exchange and that the signals of individual binding sites are broadened and time-averaged. This dynamic view of the association complex is consistent with previously measured dissociation kinetics.

The NMR data do not allow us to construct a detailed model for 27AQS2 binding to DDD because of exchange-broadened resonances, temperature-dependent line shapes, and the doubling of the signals due to a loss of symmetry. Nevertheless, clear conclusions revealing the general structure of the complexes are supported by the NMR spectral data.

The first possibility we considered was that 27AQS2 is intercalated at one of the six unique intercalation sites of DDD. Analysis of the chemical shift and NOE data for the exchangeable protons eliminates them all. For example, intercalation exclusively between A_6 and T_7 of the AATT sequence would preserve the symmetry of the complex. Inspection of Figure 3c reveals that this is not the case. Moreover, intercalation at the innermost AT site would shift the imino protons of these base pairs furthest upfield. Two protons are shifted upfield, but the NOE links at least one of them to an adjacent GC base pair, which would be impossible in this model for the innermost AT base pair. Intercalation at the neighboring A_5A_6 site can be eliminated using similar logic. In this case, the two resonances shifted upfield must be assigned to the imino protons of two AT base pairs. As is expected by intercalation at this step, the NOE data show that one upfield-shifted resonance is linked to a GC base pair while the other is linked to an unshifted AT base pair. However, an NOE is observed for the two

shifted resonances, which is not possible if the intercalated quinone separates them. By similar reasoning, binding of 27AQS2 primarily by intercalation at any of the four remaining GC base pair sites is eliminated. This does not mean that none of the quinone is intercalated, but it does indicate that the majority of it is associated with DDD nonintercalatively.

Inspection of the NOESY spectrum of the DDD−27AQS2 complex, containing the cross-peaks of the aromatic and sugar protons of the dodecamer, shows that the bases in the central AATT region of the dodecanucleotide are the most affected by complexation. For example, a T-methyl signal of this complex is shifted downfield between 0.08 and 0.35 ppm depending on its particular identity. The aromatic C6H on the perturbed T bases shows a complicated pattern of cross-peaks with the T-methyl protons. Similarly, the C6H resonance on T_8 has been split with one cross-peak negligibly upfield and one slightly downfield of the original signal. Assignment of the proton yielding the downfield NOE interaction at 7.82 ppm with the shifted T-methyl is not possible. This resonance is either an upfield-shifted C8H on A_6 or a downfield-shifted C6H on one of the T bases. Regardless of this assignment, these results are inconsistent with an intercalated quinone. In that case, we expect that most of the resonances of the complex would be shifted upfield, compared to those of the free dodecamer, just as for AQS.

Association of the tetracation with DDD causes new proton resonances to appear in the range from 6.25 to 6.85 ppm. Although certain assignment is not possible with the data available, application of the widely adopted rules which state (Hare et al., 1983) that the purine C8H or pyrimidine C6H is close enough to observe the NOE of the C1′H of its own sugar and the C1′H of an adjacent ($n - 1$) sugar suggests that these shifted resonances are the C1′H resonances from the central AT region of the dodecamer. These protons are located in the minor groove of duplex DNA.

The NMR spectral data for 27AQS2 are in accord with a predominant nonintercalative binding to the dodecamer. The temperature dependence demonstrates clearly that there is more than one complex in equilibrium in the aqueous buffer solution. Taken together, the optical and magnetic resonance spectra indicate that 27AQS2 binds primarily to the minor groove of DDD in the central AATT region. A model for the tetracation associated in this fashion is shown in Figure 6. This model was constructed by docking 27AQS2, minimized by a molecular mechanics calculation, into the standard B-form DNA of this dodecamer. No attempts were made to minimize the ensemble, and thus, the structure is meant to be figurative rather than definitive. Clearly, however, a comfortable fit of 27AQS2 in the minor groove of DNA with the tetracationic arms pointing away from the bases can be generated. In this orientation, each of the positively charged ammonium groups can be placed within van der Waals contact of a negatively charged phosphate group. This arrangement of the ionic charges maximizes the electrostatic stabilization of the complex and may explain why AQS intercalates while 27AQS2 does not. The AT rich regions of DNA are considered to be better sites than GC regions for binding of positively charged ligands, like 27AQS2, because they have a higher negative electrostatic potential (Pullman & Pullman, 1981). Clearly, van der Waals and hydrogen bonding interactions may also play important roles in determining the binding site.

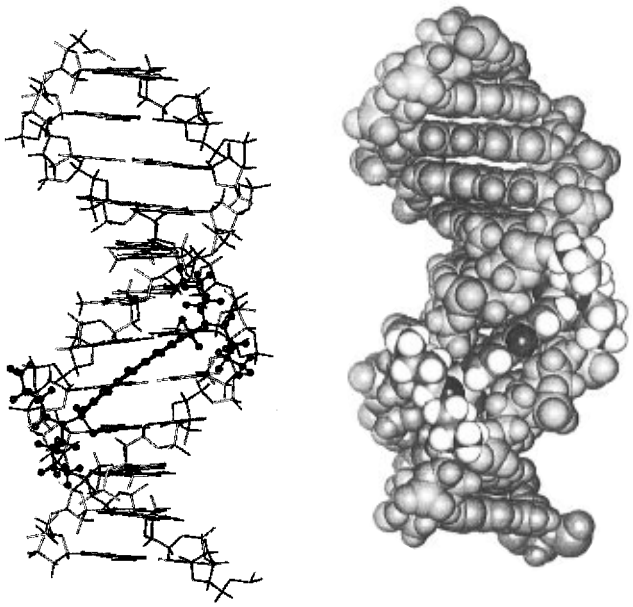

FIGURE 6: Space filling depiction of the minor groove-bound complex of 27AQS2 with the central AATT region of DDD. The structure of this complex has not been minimized and is meant to be illustrative, not definitive.

(2) Reactions of Excited State Anthraquinones Associated with DNA. The structure of the complex of the anthraquinone derivative with DNA will affect its photochemistry and photophysics. We have shown that photoinduced electron transfer from an electron rich base dominates the chemistry of intercalated quinones. Laser flash photolysis studies of intercalated quinones reveal products from the quenching of the anthraquinone excited state by electron transfer (Armitage et al., 1994; Breslin & Schuster, 1996; Ly et al., 1996). This reaction is facilitated by strong π-electron overlap of the anthraquinone with a nucleic acid base. The intimate electronic coupling of the anthraquinone with DNA, expected to give rise to fast and efficient electron transfer, is further shown by the induced shifts in the absorption spectrum of the complex. Quantitative phosphorescence quenching of the intercalated anthraquinones is also a clear demonstration that electron transfer is efficient.

A groove-bound anthraquinone, like 27AQS2, resides in a completely different chemical environment. A groove-bound quinone has poor π-electron overlap with the nucleic acid bases, a circumstance that will retard the rate of photoinduced electron transfer. The weaker orbital overlap of 27AQS2 with the nucleotides can be seen in the absorption spectra of the complex. The smaller hypochromic effect of the tetracation is consistent with this view. Furthermore, since the phosphorescence results indicate that the rate of photoinduced electron transfer is reduced, competing unimolecular photophysical processes can be more efficient. Indeed, 27AQS2 shows incomplete phosphorescence quenching with DNA, especially with poly(dA)·poly(dT).

We have shown that the light-induced cleavage of the 5′-G of GG steps in DNA by intercalated quinones is initiated by electron transfer (Breslin & Schuster, 1996). Localization of the radical cation (hole) at the GG step, the most easily oxidized sequence (Sugiyama & Saito, 1996), and subsequent reaction with water or O_2 lead to DNA damage. Other

organic photosensitizers such as nitroaromatic compounds (Iverson, 1988), naphthalimide (Siato et al., 1995; Siato & Takayama, 1995), riboflavin (Ito et al., 1993), and benzophenone derivatives (Takayama, 1995) can serve as excited state one-electron oxidants of DNA that cause GG selective cleavage. Comparison of ALD cleavage by AQS and 27AQS2 shows that both quinones, within experimental error, yield the same selectivity for the 5′-G cleavage. However, the efficiency of DNA scission by the tetracation is much lower than for intercalated AQS. This indicates that electron transfer from the groove-bound 27AQS2 is either very slow or impossible and that the observed cleavage arises either by this route or from a small fraction of intercalated 27AQS2.

CONCLUSION

Modest structural modification of anthraquinones with appended flexible ammonium side chains leads to a change in the binding mode and a concomitant change in the photochemical reactivity. The monocationic and dicationic anthraquinone derivatives are shown to be DNA intercalators. The tetracationic quinone, 27AQS2, is bound in the minor groove of duplex DNA. Spectroscopic analysis, particularly ^{1}H NMR spectroscopy, suggests that 27AQS2 binds in an AT rich region of a synthetic dodecanucleotide. Irradiation of intercalated quinones causes rapid electron transfer, leading to selective cleavage at the 5′-G of GG steps. Electron transfer from the nucleic acid bases to excited 27AQS2 is less efficient and so is the cleavage of the DNA.

EXPERIMENTAL PROCEDURES

Materials. Ethidium bromide and propidium iodide were obtained as solutions from Molecular Probes. DNA polymers poly(dAdT)$_2$, poly(dGdC)$_2$, and poly(dA)·poly(dT) were purchased from Pharmicia Biotech and were used as received. The concentrations quoted are in base pairs and were determined by UV measurements. 2,7-Anthraquinonedisulfonic acid and 2-anthraquinonesulfonic acid were purchased from Aldrich. Dodecamer DDD was prepared and purified by N. Boguslavsky of the School of Chemistry and Biochemistry (Georgia Institute of Technology).

Instrumentation. UV spectra were recorded on a Cary-1E spectrophotometer. CD spectra were recorded on a Jasco-720 instrument. The fluorescence binding titrations and phosphorescence spectra were recorded on a SPEX 1681 Fluorolog instrument. NMR spectral characterization of the anthraquinones was performed on a Nicolet QE-300 spectrometer. NMR spectral studies of the oligomer−anthraquinone complexes were obtained on a Varian Unity+ 500 MHz instrument. Elemental analyses were performed at the University of Illinois Microanalysis Service Laboratory.

NMR Spectral Studies. DDD (6.6 mg) was dissolved in 1 mL of a buffer solution containing 100 mM NaCl and 10 mM sodium phosphate at pH 7 (this buffer is referred to herein as PBS). Aliquots (0.33 mL) of this solution were placed in individual NMR tubes. One tube was diluted with 0.6 mL of PBS. Solutions containing the anthraquinones were added to other aliquots, and the resulting solutions were diluted with additional PBS to give a total volume of 0.6 mL. The solvent for samples used in measurements of the nonexchangeable protons was exchanged with D_2O by three successive cycles of evaporation followed by re-dissolution with 0.6 mL of D_2O. Samples used for determination of the exchangeable proton spectra were prepared by three successive evaporation−H_2O hydration cycles followed by final dissolution with 85% H_2O−15% D_2O. The chemical shift standard used for all samples was 0.1% TSP.

The spectra were recorded with a Varian Unity+ 500 MHz spectrometer on a nonspinning sample into 128K data points over a spectral width of 10 kHz. Each spectrum consisted of 128 transients acquired with a 3 s recycle delay, during which the HOD resonance was suppressed by low-power irradiation. Spectra recorded in 85% H_2O/15% D_2O were collected with a 2 s presaturation period. A non-water excitation suppression scheme was used. Data were acquired over a 12 kHz spectral width into 128K data points.

NOESY data were collected on the Varian Unity+ 500 MHz spectrometer using the procedure previously described (Parkinson, 1994). The two-dimensional data were collected into 4056 complex data points; 128 transients were recorded for each free induction decay. Data were collected over a 14 kHz spectral width using a 1.5 s recycle delay and a 170 ms mixing time.

Irradiation Conditions. Samples (10 μL each) were irradiated for 30 min at 350 nm in a Rayonet Photoreactor equipped with four 15 W lamps. The samples were contained in 1.5 mL Eppendorf centrifuge tubes.

Bis[3-[N-(1-butoxycarbonyl)amino]propyl]amine Hydrochloride. To a solution of 11.0 g (84 mmol) of 1,7-diamino-4-azaheptane in 400 mL of a 3:1 methanol/water mixture was added slowly a solution containing 33 g of di-*tert*-butoxycarbonate in 220 mL of 90% methanol/water. The reaction mixture was stirred for 16 h and then the volume reduced to approximately 200 mL. The pH was adjusted to 12.5 with KOH, and the solution was extracted several times with diethyl ether (2 L total volume). The ether extract was dried over $MgSO_4$ and evaporated to dryness. The residue was dissolved in 100 mL of methanol, and the pH was adjusted to 5.3 with HCl. Then, 300 mL of water was added, and the resulting solid was removed by filtration. The filtrate was concentrated to dryness and the product recrystallized from methanol and ether yielding 13.0 g of colorless plates: mp 172 °C (dec); ^{1}H NMR ($CDCl_3$) δ 1.43 (s, 18 H), 1.58 (s, 2 H), 2.08 (t, J = 6.2 Hz, 4 H), 2.97 (q, J = 6.2 Hz, 4 H), 3.32 (q, J = 6.2 Hz, 4 H), 5.27 (s, 2 H); ^{13}C NMR δ 26.38, 29.15, 36.65, 45.18, 79.82, 158.03.

N-[3-[N-(tert-Butoxycarbonyl)amino]propyl]-2-anthraquinonesulfonamide (Boc-protected 2AQS) was prepared in 83% yield by the reaction of 0.59 g (1.63 mmol) of 2-anthraquinonesulfonyl chloride and 0.34 g (1.72 mmol) of *N*-(1-butoxycarbonyl)-1,3-diaminopropane hydrochloride in triethylamine (5 mL) and dichloromethane (150 mL): mp 113−115 °C; ^{1}H NMR ($CDCl_3$) δ 1.35 (s, 9 H), 1.65 (q, J = 6.0 Hz, 2 H), 3.07 (q, J = 6.0 Hz, 2 H), 3.21 (q, J = 6.0 Hz, 2 H), 4.65 (t, J = 6.0 Hz, 1 H), 6.13 (t, J = 6.0 Hz, 1 H), 7.82−7.89 (m, 2 H), 8.25−8.37 (m, 2 H), 8.44 (d, J = 8.1 Hz, 1 H), 8.78 (d, J = 1.5 Hz, 1 H); ^{13}C δ 28.03, 30.37, 36.56, 39.80, 80.77, 126.00, 127.64, 128.57, 131.98, 133.31, 133.37, 134.14, 134.83, 146.30, 160.61, 182.0, 182.29. Anal. Calcd for $C_{22}H_{24}O_6N_2S$: C, 59.45; H, 5.44; N, 6.30. Found: C, 59.32; H, 5.48; N, 6.27.

N,N′-Bis[3-[N-(tert-butoxycarbonyl)amino]propyl]-2,7-anthraquinonedisulfonamide (Boc-protected 27AQS) was prepared in 67% yield by the reaction of 0.5 g (1.23 mmol) of 2,7-anthraquinonedisulfonyl chloride and 0.53 g (2.52 mmol) of *N*-(1-butoxycarbonyl)-1,3-diaminopropane hydrochloride

in triethylamine (6 mL) and dichloromethane (150 mL), following the previously described procedure (Armitage et al., 1994): mp 182−183 °C; ^{1}H NMR ($CDCl_3$) δ 1.36 (s, 18 H), 1.65 (q, J = 5.7 Hz, 4 H), 3.08 (q, J = 5.7 Hz, 4 H), 3.22 (q, J = 5.7 Hz, 4 H), 4.65 (t, J = 5.7 Hz, 2 H), 6.22 (t, J = 5.7 Hz, 2 H), 8.31 (dd, J = 8.1, 1.8 Hz, 2 H), 8.46 (d, J = 8.1 Hz, 2 H), 8.80 (d, J = 1.9 Hz, 2 H); ^{13}C NMR δ 28.00, 30.46, 36.48, 42.34, 79.91, 126.17, 126.22, 128.83, 132.35, 133.92, 135.31, 180.65, 186.63. Anal. Calcd for $C_{30}H_{40}N_{40}O_{12}S_2$: C, 52.93; H, 5.92; N, 8.23. Found C, 52.93; H, 6.00; N, 7.97.

N,N,N′,N′-Tetrakis[3-[N-(tert-butoxycarbonyl)amino]-propyl]-2,7-anthraquinonedisulfonamide (Boc-protected 27AQS2) was prepared in 80% yield by the reaction of 0.5 g (1.23 mmol) of 2,7-anthraquinonedisulfonyl chloride and 0.93 g (2.53 mmol) of bis[3-[*N*-(1-butoxycarbonyl)amino]-propyl]amine hydrochloride in triethylamine (6 mL) and dichloromethane (150 mL), following the previously described procedure (Armitage et al., 1994): mp 174 °C (dec); ^{1}H NMR ($CDCl_3$) δ 1.43 (s, 36 H), 1.76 (q, J = 6.9 Hz, 8 H), 3.15−3.20 (m, 8 H), 3.26 (t, J = 6.9 Hz, 8 H), 4.91 (s, 4 H), 8.24 (dd, J = 8.1, 1.5 Hz, 2 H), 8.49 (d = 8.1 Hz, 2 H), 8.71 (d, J = 1.5 Hz, 2 H); ^{13}C NMR δ 28.14, 29.10, 46.06, 63.71, 79.37, 126.21, 129.11, 132.45, 134.16, 135.56, 145.76, 156.33, 180.72, 181.10. Anal. Calcd for $C_{46}H_{70}N_6S_2O_{14}\cdot H_2O$: C, 54.53; H, 7.16; N, 8.29. Found: C, 54.90; H, 7.12; N, 7.95.

N-(3-Aminopropyl)-2-anthraquinonesulfonamide hydrochloride (AQS) was prepared in 90% yield from 0.30 g (0.67 mmol) of *N*-[3-[*N*-(*tert*-butoxycarbonyl)amino]propyl]-2-anthraquinonesulfonamide following the previously described procedure (Armitage et al., 1994): mp 232 °C (dec); ^{1}H NMR (D_2O) δ 1.91 (q, J = 6.9 Hz, 2 H), 3.08−3.14 (m, 4 H), 4.80 (s, 4 H), 7.81−7.84 (m, 2 H), 7.98−8.02 (m, 2 H), 8.16 (s, 2 H), 8.34 (s, 1 H); ^{13}C NMR δ 27.40, 36.35, 39.43, 124.87, 125.93, 127.29, 128.60, 132.03, 133.37, 134.14, 132.25, 135.25, 135.43, 135.71, 145.83, 182.14, 182.23. Anal. Calcd for $C_{17}H_{17}N_2O_4Cl$: C, 53.62; H, 4.50; N, 7.36; Cl, 9.31. Found: C, 53.28; H, 4.54; N, 7.36; Cl, 9.71.

N,N′-Bis(3-aminopropyl)-2,7-anthraquinonedisulfonamide dihydrochloride (27AQS) was prepared in 86% yield from 0.26 g (0.038 mmol) of *N,N′*-bis[3-[*N*-(*tert*-butoxycarbonyl)amino]propyl]-2,7-anthraquinonedisulfonamide following the previously described procedure: mp 220 °C (dec); ^{1}H NMR (DMSO-d_6) δ 1.69 (q, J = 7.2 Hz, 4 H), 2.71−2.79 (m, 4 H), 2.89 (q, J = 7.2 Hz, 4 H), 7.99 (s, 6 H), 8.28−8.34 (m, 4 H), 8.41 (d, J = 8.1 Hz, 2 H), 8.54 (s, 2 H); ^{13}C NMR δ 26.24, 36.33, 45.78, 125.09, 132.49, 134.34, 135.98, 144.33, 155.53, 181.26, 181.76. Anal. Calcd for $C_{20}H_{26}N_4O_6S_2Cl_2$: C, 43.41; H, 4.74; N, 10.12. Found: C, 43.76; H, 4.92; N, 9.71.

N,N,N,N′-Tetrakis(3-aminopropyl)-2,7-anthraquinonedisulfonamide tetrahydrochloride (27AQS2) was prepared in 87% yield from 0.39 g (0.38 mmol) of *N,N,N′,N′*-tetrakis-[[*N*-(1-butoxycarbonyl)amino]propyl]-2,7-anthraquinonedisulfonamide following the previously described procedure (Armitage et al., 1994): mp 229 °C (dec); ^{1}H NMR (D_2O) δ 1.98 (q, J = 7.2 Hz, 8 H), 3.07 (t, J = 7.2 Hz, 8 H), 3.38 (t, J = 7.2 Hz, 8 H), 4.80 (s, 12 H), 8.24−8.32 (m, 4 H), 8.46 (s, 2 H); ^{13}C NMR δ 27.40, 37.49, 46.97, 126.26, 130.16, 137.14, 145.49, 154.18, 182.23, 182.53. Anal. Calcd for $C_{26}H_{42}N_6S_2O_6Cl_4\cdot H_2O$: C, 41.12; H, 5.85. Found: C, 41.36; H, 6.23.

ACKNOWLEDGMENT

The authors are especially grateful for the assistance provided by Dr. L. Gelbaum of the Georgia Institute of Technology in collecting the NMR data. We thank Dr. N. Boguslavsky for preparing the DNA dodecamer. We also thank Mr. Y. Kan for the stopped-flow measurement of the DNA dissociation rate of 27AQS2. The high-field NMR studies of the anthraquinone−dodecamer complexes were completed at the NIH-funded NMR facility at Georgia State University.

REFERENCES

Armitage, B., & Schuster, G. B. (1997) *Photochem. Photobiol.* (in press).
Armitage, B., Yu, C., Devadoss, C., & Schuster, G. B. (1994) *J. Am. Chem. Soc. 116*, 9847−9859.
Barton, J. K. (1986) *Science 233*, 727.
Breiner, K. M., Daugherty, M. A., Oas, T. G., & Thorp, H. H. (1995) *J. Am. Chem. Soc. 117*, 11673−11679.
Breslin, D. T., & Schuster, G. B. (1996**)** *J. Am. Chem. Soc. 118*, 2311−2319.
Breslin, D. T., & Schuster, G. B (1997) *J. Am. Chem. Soc. 119* (in press).
Brun, A. M., & Harriman, A. (1992) *J. Am. Chem. Soc. 114*, 3656.
Cadet, J., Berger, M., Decarroz, C., Wagner, J. R., Van Lier, J. E., Ginot, Y. M., & Vigny, P. (1986) *Biochimie 68*, 813.
Cheng, C.-C., Goll, J. G., Neyhart, G. A., Welch, T. W., Singh, P., & Thorp, H. H. (1995) *J. Am. Chem. Soc. 117*, 2970.
Coury, J., Williams, L., Bottemley, L. A., Breslin, D. T., & Schuster, G. B. (1997) *J. Am. Chem. Soc.* (submitted for publication).
Cullis, P. M., Malone, M. E., & Merson-Davies, L. A. (1996) *J. Am. Chem. Soc. 118*, 2775.
Dizdaroglu, M. (1984) *J. Chromatogr. 295*, 103.
Eriksson, M., Leijon, M., Hiort, C., Nordén, B., & Gräslund, A. (1994) *Biochemistry 33*, 5031−5040.
Floyd, R. A., West, M. S., Eneff, K. L., & Schneider, J. E. (1989) *Arch. Biochem. Biophys. 273*, 106.
Gräslund, A., & Leijon, M. (1992) *Nucleic Acids Res. 20*, 5339−5343.
Hall, D. B., Holmlin, R. E., & Barton, J. K. (1996) *Nature 382*, 731.
Hare, D. R., Wemmer, D. E., Drobny, G., & Reid, B. R. (1983) *J. Mol. Biol. 171*, 319−336.
Hertzberg, R. P., & Dervan, P. B. (1982) *J. Am. Chem. Soc. 104*, 313.
Hertzberg, R. P., & Dervan, P. B. (1984) *Biochemistry 23*, 3934.
Ito, K., Inoue, S., Yamamoto, K., & Kawanishi, S. (1993) *J. Biol. Chem. 268*, 13221−13227.
Iverson, B. L. (1988) Ph.D. Thesis, California Institute of Technology, Pasadena, CA.
Jeppesen, C., & Nielsen, P. E. (1988) *Nucleic Acids Res. 17*, 4947−4959.
Jovanovic, S. V., & Simic, M. G. (1986) *J. Phys. Chem. 90*, 976.
Koch, T., Ropp, J. D., Sligar, S. G., & Schuster, G. B. (1993) *Photochem. Photobiol. 58*, 554−558.
Liang, G., Gannett, P., Shi, X., Zhang, Y., Chen, F.-X., & Gold, B. (1994) *J. Am. Chem. Soc. 116*, 1131.
Ly, D., Kan, Y., Armitage, B., & Schuster, G. B. (1996) *J. Am. Chem. Soc. 118*, 1847−1848.
Lyng, R., Roger, A., & Nordèn, B. (1991a) *Biopolymers 31*, 1709−1720.
Lyng, R., Roger, A., & Nordèn, B. (1991b) *Biopolymers 32*, 1201−1214.
Nagai, K., Carter, B. J., Xu, J., & Hecht, S. M. (1991) *J. Am. Chem. Soc. 113*, 5099.
Nelson, H. C. M., Sinch, D. T., Luisi, B. F., & Klug, A. (1987) *Nature 330*, 211−226.
Neyhart, G. A., Grover, N., Smith, S. R., Kalsbeck, W. A., Fairley, T. A., Cory, M., & Thorp, H. H. (1993) *J. Am. Chem. Soc. 115*, 4423.
Nicolau, K. C., Maligres, P., Shin, J., de Leon, E., & Rideout, D. (1990) *J. Am. Chem. Soc. 112*, 7825.

Nielsen, P. E. (1991) *Bioconjugate Chem. 2*, 1.
Nielsen, P. E., Hiort, C., Sonnichsen, S. H., Buchardt, O., Dahl, O., & Nordén, B. (1992) *J. Am. Chem. Soc. 114*, 4967−4975.
Papavassiliou, A. G. (1995) *Biochem. J. 305*, 345.
Parkinson, J. A., Ebrahimi, S. E., McKie, J. H., & Douglas, K. T. (1994) *Biochemistry 33*, 8442−8452.
Patel, D. J., Kozlowski, S. A., Rice, J. A., Broka, C., & Itakura, K. (1981) *Proc. Natl. Acad. Sci. U.S.A. 78*, 7281−7284.
Phillips, D. R., & Roberts, G. C. K. (1980) *Biochemistry 21*, 4795.
Pratviel, G., Bernadou, J., & Meunier, B. (1995) *Angew. Chem., Int. Ed. Engl. 34*, 746−769.
Pullman, A., & Pullman, B. (1981) *Q. Rev. Biophys. 14*, 289−380.
Ranganathan, D., Patel, B. K., & Mishra, R. K. (1994) *J. Chem. Soc., Chem. Commun.* 107.
Raoul, S., & Cadet, J. (1996) *J. Am. Chem. Soc. 118*, 1892.
Riordan, C. G., & Wei, P. (1994) *J. Am. Chem. Soc. 116*, 2189.
Saito, I., Takayama, M., & Matsuura, T. (1990) *J. Am. Chem. Soc. 112*, 883.
Saito, I., Takayama, M., Sugiyama, M., & Nakatani, K. (1995) *J. Am. Chem. Soc. 117*, 6406.
Schnaith, L. M. T., Hanson, R. S., & Que, L., Jr. (1994) *Proc. Natl. Acad. Sci. U.S.A. 91*, 569.
Sheu, C., & Foote, S. C. (1995) *J. Am. Chem. Soc. 117*, 6439.
Siato, I., & Takayama, M. (1995) *J. Am. Chem. Soc. 117*, 5590−5591.
Siato, I., Takayama, M., Sugiyama, H., & Nakatani, K. (1995) *J. Am. Chem. Soc. 117*, 6406−6407.
Siebenlist, U., Simpson, R. B., & Gilbert, W. (1980) *Cell 20*, 269.
Sigman, D. S. (1986) *Acc. Chem. Res. 19*, 180.
Sigman, D. S., Mazumder, A., & Perrin, D. M. (1993) *Chem. Rev. 93*, 2295−2316.
Sitlani, A., Long, E. C., Pyle, A. M., & Barton, J. K. (1992) *J. Am. Chem. Soc. 114*, 2303−2312.
Stubbe, J., & Kozarich, J. W. (1987) *Chem. Rev. 87*, 1107.
Sugiyama, H., & Saito, I. (1996) *J. Am. Chem. Soc. 118*, 7063−7068.
Takasaki, B. K., & Chin, J. (1994) *J. Am. Chem. Soc. 116*, 1121.
Takayama, M. (1995) Ph.D. Thesis, Kyoto University, Kyoto, Japan.
Tullius, T. D., Dombroski, B. A., Churchill, M. E. A., & Kam, L. (1987) *Methods Enzym*ol. *155*, 537.
Uchida, K., Pyle, A. M., Morii, T., & Barton, J. K. (1989) *Nucleic Acids Res. 17*, 10259.
Wilson, W. D., Tanious, F. A., Barton, H. J., Strekowski, L., & Boykin, D. W. (1989a) *J. Am. Chem. Soc. 111*, 5008−5010.
Wilson, W. D., Tanious, F. A., Watson, R. A., Barton, H. J., Strekowska, A., Harden, D. B., & Strekowski, L. (1989b) *Biochemistry 28*, 1984−1992.
Wilson, W. D., Tanious, F. A., Barton, H. J., Jones, R. L., Fox, K., Wydra, R. L., & Strekowski, L. (1990) *Biochemistry 29*, 8452.

BI9702750